ACS OMEGA

http://pubs.acs.org/journal/acsodf

Article

New Chitosan-Grafted Thymol Coated on Gold Nanoparticles for Control of Cariogenic Bacteria in the Oral Cavity

Pakawat Chittratan, Jongjit Chalitangkoon, Karn Wongsariya, Arjnarong Mathaweesansurn, Ekarat Detsri,* and Pathavuth Monvisade*

Cite This: *ACS Omega* 2022, 7, 26582−26590

Read Online

ACCESS | Metrics & More | Article Recommendations | Supporting Information

ABSTRACT: Chitosan-grafted thymol (CST) coated on gold nanoparticles has been synthesized and characterized for the design of antimicrobial materials. CST was synthesized via adapting the Mannich reaction, and it acted as the capping agent for the synthesis of gold nanoparticles (AuNPs). The grafting of thymol onto the side chain of chitosan has provided a degree of substitution value ($\%DS_{NMR}$) of 10.0%, calculated by nuclear magnetic resonance spectroscopy. UV−visible spectrometry and elemental analysis were used to confirm the successful synthesis of CST through adapting the Mannich reaction. The appropriate concentration of CST for AuNP synthesis was found to be 0.020% w/v. A red-wine colloidal AuNP solution of 2.41−3.30 nM particle size exhibits a strong surface plasmon resonance at 502 nm, which shows negative charges at pH = 9 of −36.37 mV. This result evidenced that the AuNPs showed electrostatic repulsion and CST played a role as a capping agent to provide a good dispersion and stability state. CST coated on the AuNP surface was successfully utilized for the control of cariogenic bacteria in the oral cavity. The results obtained from this study show that the tuning of the capping agent used in the synthesis step strongly influences the latter antimicrobial activity of the nanoparticles against *Streptococcus mutans* ATCC 25175 and *Streptococcus sobrinus* ATCC 33402 activity, with an inhibition zone of 15.90 and 14.25 mm, respectively. The average minimum inhibitory concentration values against *S. mutans* ATCC 25175 and *S. sobrinus* ATCC 33402 were found to be 25 and 100 mg/L, respectively, whereas the minimum bactericidal concentration values were 100 and 200 mg/L, respectively.

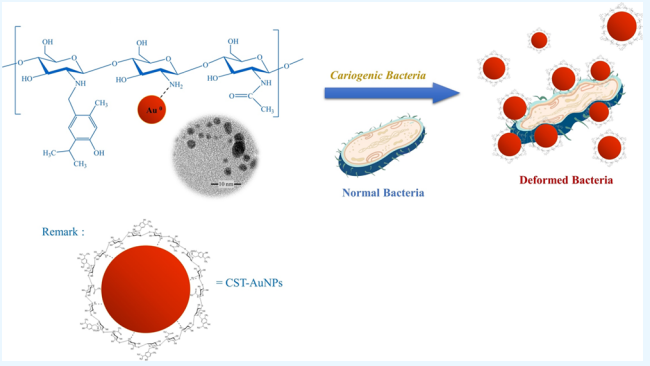

1. INTRODUCTION

Some oral infections including cavities, gingivitis, and periodontal disease are common from childhood to adulthood. Cavities are one of the most common oral infections caused by the bacteria *Streptococcus mutans* (*S. mutans*) and *Streptococcus sobrinus* (*S. sobrinus*), one of the principal cariogenic dental biofilm inhabitants that feeds on sugary, sticky foods, and beverages. *S. mutans* and *S. sobrinus* secrete glucosyltransferase on its cell wall, which allows the bacteria to produce polysaccharides from sucrose. These sticky polysaccharides are responsible for the bacteria's ability to aggregate with one another and adhere to tooth enamel.[1,2] To prevent the oral infections, daily brushing, flossing, and the use of appropriate mouthwash can significantly reduce the number of oral bacteria. Three different types of clinically used and most frequently studied antiplaque agents are sodium fluoride, ampicillin, and chlorhexidine.[1,3] However, some inherent issues of these antiplaque agents could not be avoided such as brown staining of the teeth and tongue, an unpleasant taste, enhanced supragingival calculus formation, and rarely painful desquamations of the oral mucosa all of which have led to the search for new formulations. Recently, gold nanoparticles (AuNPs) have been proposed as an antimicrobial agent to prevent the oral infections.[4−6] Most of the published work has mainly focused on the preparation of AuNPs conjugated with antibiotics, antimicrobial peptides, and ligands[4,7−12] in order to enhance the antibacterial abilities. AuNPs with smaller sizes have various benefits in antibiotic delivery such as regulating size and morphology, high-density surface ligands, and delivery without losing drugs which protects them from destruction. Darabpour et al.,[13] developed AuNPs using the chemical reduction technique and immobilized methylene blue onto AuNP surface. The particle sizes of AuNPs and zeta potential were found to be 85 nm and +32 mV, respectively. AuNPs conjugated with methylene blue demonstrated important photoinactivation across *Staphylococcus aureus* (*S. aureus*) biofilms. A reduction of greater than $5\log_{10}$ CFU was found.

Received: May 5, 2022
Accepted: July 11, 2022
Published: July 19, 2022

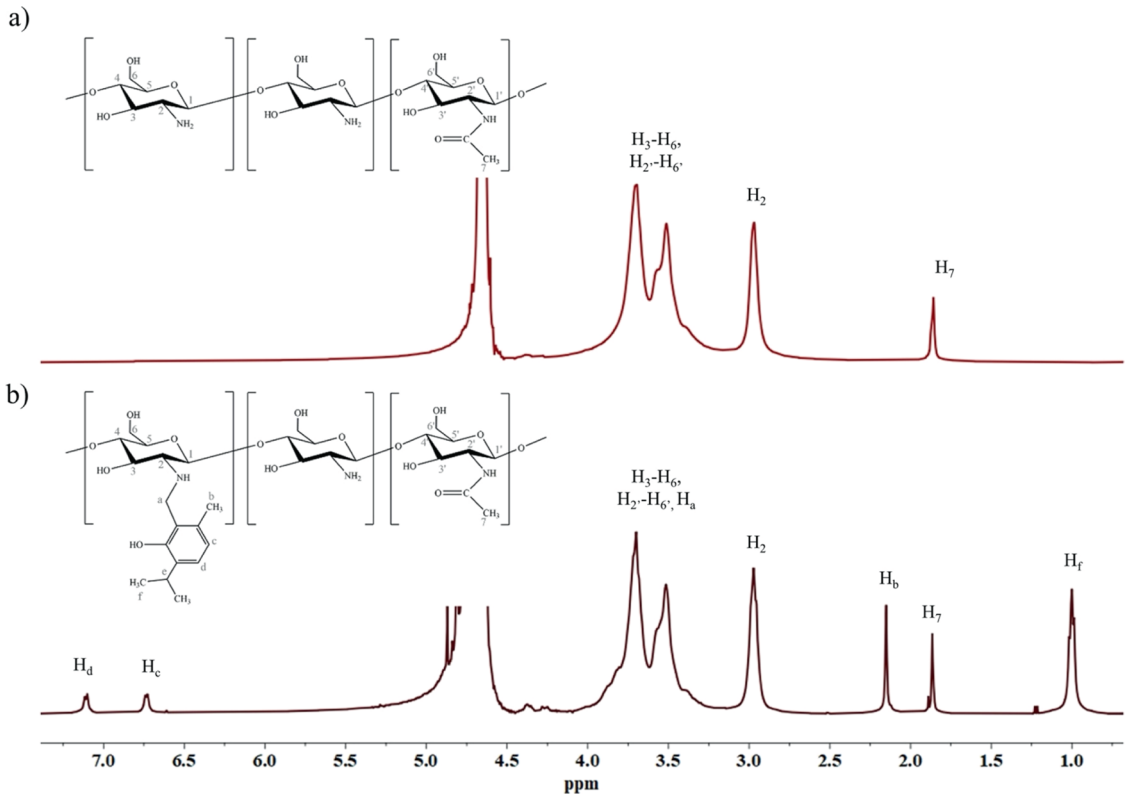

Figure 1. ^{1}H NMR spectra of (a) chitosan and (b) CST in CF_3COOH/D_2O.

Singh et al.,[14] explored the aqueous extract of *C. sativa* to synthesized AuNPs without any additional reducing and capping agents. The synthesized AuNPs were crystalline with an average diameter of 12−18 nm and showed bactericidal effects against *Pseudomonas aeruginosa* and *Escherichia coli*. Jiang and co-workers[15] fabricated AuNPs with 4,6-diamino-2-pyrimidinethiol in order to kill *Escherichia coli* ATCC11775 (*E. coli*) with multidrug-resistance Gram-negative bacteria efficiency to induce drug resistance to a much smaller degree than conventional antibiotics.

In this research, we have performed synthesis and characterization of chitosan-grafted thymol (CST) on the AuNP surface for antimicrobial activities in the oral cavity. It is well known that chitosan[16−19] and thymol[20−22] are most frequently used for antimicrobial and antiplaque agents. Chitosan has received much more attention as a chemical agent for mouthwashes that provides clinical benefits for plaque control. Chitosan is a linear polysaccharide composed of randomly distributed β-linked D−glucosamine and N−acetyl−D−glucosamine. The protonated amino groups upon chitosan chains interact with bacterium cell walls negatively charged, disrupting them and providing microbial death. Various methods have been tried to improve its antibacterial activity either by a physical or chemical strategy. Chemical modification requires introducing new groups onto the backbone by reacting with hydroxyl or with amino groups such as saccharization, alkylation, acylation, quaternization, and metallization.[23−27] These modifications bring chitosan a better antibacterial activity and expand its application as well with *S. aureus* and *E. coli*. However, there are a few research studies on the effects of chitosan derivatives against *S. mutans* and *S. sobrinus* especially for oral application. For this reason, the objective was to designed chitosan modified with thymol via adapting the Mannich reaction to enhance the antimicrobial properties and use them as a capping agent for AuNP synthesis. Many characterization techniques, such as UV−visible spectrometry, X-ray diffraction (XRD), transmission electron microscopy (TEM), zeta potential analyzer elemental analysis (EA), and ^{1}H NMR, were used to confirm the successful synthesis of CST and AuNPs. Finally, CST coated on gold nanoparticles was applied as the antimicrobial agent to control the growth of bacteria in oral application.

2. EXPERIMENTAL SECTION

2.1. Chemicals. High-molecular-weight chitosan (320,000 Da) was purchased from Eland Co., Ltd. (Bangkok, Thailand). The percentage of degree of deacetylation (%DD) of chitosan (CS) is 85%. Formaldehyde (HCHO: 37% w/w), hydrochloric acid (HCl), and sodium hydroxide (NaOH) were purchased form Carlo Erba (Italy). Thymol ($C_{10}H_{14}O$), gold(III) chloride trihydrate ($HAuCl_4{\cdot}3H_2O$), and sodium borohydride ($NaBH_4$) were acquired from Sigma-Aldrich Germany. All chemicals are of analytical reagent grade (AR grade) and used without further purification. Ultrapure deionized water (Milli−Q ultrapure water) with a resistivity of 18.2 MΩ cm at 25 °C was used for preparing all chemical solutions.

2.2. Preparation of CST. CST was synthesized by a well-described method through the Mannich reaction adapted from our previous research.[28] The preparation steps can be summarized as follows: chitosan (1 g) was dissolved in 100 mL of 1% w/v acetic acid solution under vigorous stirring. Then, 0.7932 g of thymol dissolved in 10 mL of dimethylformamide and 0.2147 g of formaldehyde were slowly dropped into chitosan solution and stirred at 60 °C for 24 h. After that, 0.5 M of fresh NaOH solution was added into the solution mixture for precipitation. The mixture was then

https://doi.org/10.1021/acsomega.2c02776
ACS Omega 2022, 7, 26582−26590

Scheme 1. Schematic Illustration of the Synthesis of (a) CST and (b) CST Coated on the Gold Nanoparticle Surface

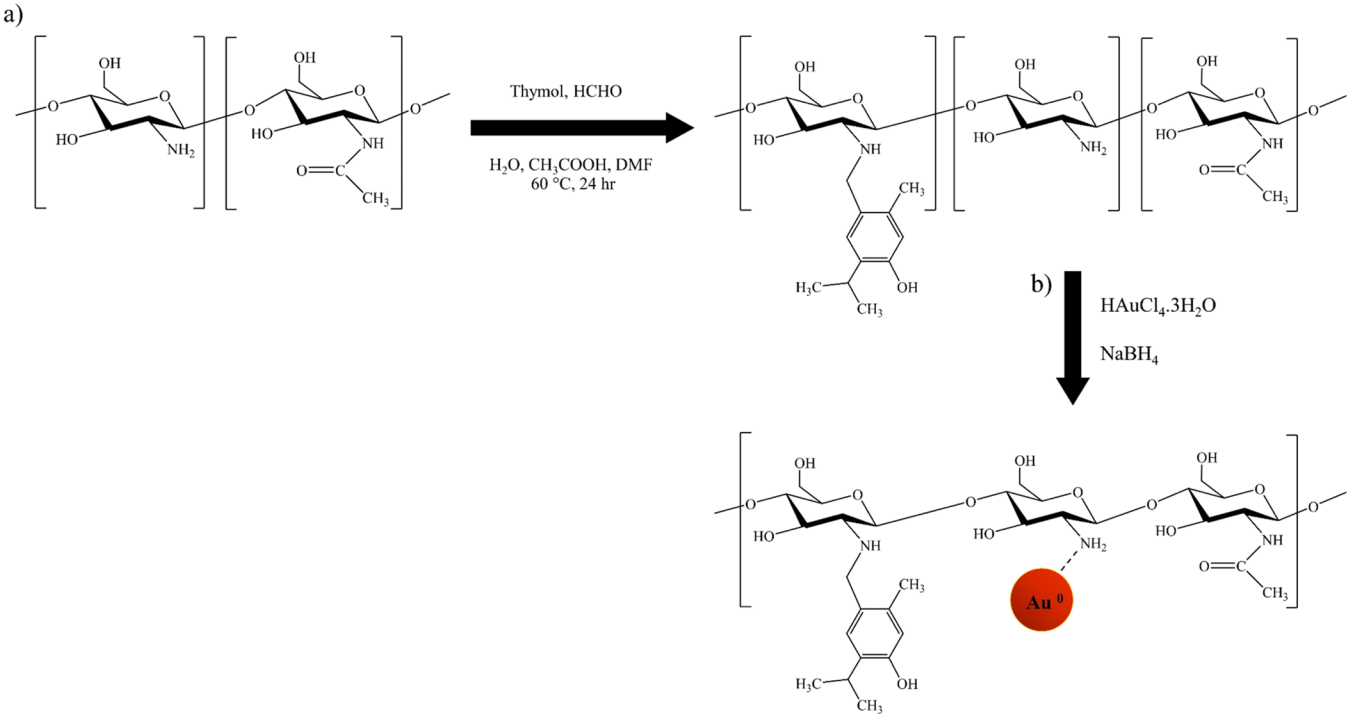

filtered using filter paper and washed with ethanol and distilled water. The precipitate was dried at 60 °C to obtain a CST product.

The structural characterization of CST was performed by ^{1}H NMR, EA, and UV−vis spectroscopy techniques. The UV−vis spectra were scanned from 200−800 nm using a BlueStar B spectrophotometer (Lab Tech, China). The ^{1}H NMR spectra were determined using a JNM-ECZ-500R/S1 spectrometer (JEOL, Japan) at 500 MHz. D_2O/CF_3COOH was used to dissolve CST. The degree of substitution (%DS) determination of CST was calculated using ^{1}H NMR and EA followed eqs 1 and 2, respectively.

$$\%DS_{NMR} = \frac{\left(\frac{H_f}{6}\right)}{H_2} \times 100 \quad (1)$$

where %DS is the degree of substitution percentage, and H_f and H_2 are the integral areas of protons indicated in Figure 1.

$$\%DS_{EA} = \left(\frac{\left(\frac{C}{N}\right)_D - \left(\frac{C}{N}\right)_O}{n}\right) \times \frac{14}{12} \times 100 \quad (2)$$

where $\%DS_{EA}$ is the degree of substitution percentage obtained from EA data; $(C/N)_D$ is the carbon to nitrogen mass ratios of the chitosan derivative; and $(C/N)_O$ is the carbon to nitrogen mass ratios of the original chitosan.

2.3. Synthesis of CST Coated on Gold Nanoparticles. AuNPs were synthesized by chemical reduction using CST and $NaBH_4$ as the capping and reducing agents, respectively. Briefly, 10 mL of 10 mM $HAuCl_4{\cdot}3H_20$ was mixed with 0.1% w/v of CST. Then, an aliquot of 0.5 mL $NaBH_4$ (50 mmol/L) was rapidly added to a solution mixture under stirring for 10 min at 25 °C. The color of the solution was changed rapidly from light yellow to red-wine immediately. The stirring process was continued for 30 min to complete reduction and homogenization. Finally, the dark red solution of CST−AuNPs with pH 9.0 was obtained. The synthesized solution was purified with a dialysis tube and stored at 4 °C in a refrigerator for 24 h before further use.

To estimate the concentration of CST−AuNPs, the stock colloidal CST−AuNP solution was diluted three times using ultrapure water, and the absorbance intensity was measured at λ_{max} = 502 nm using UV−vis spectrometry. The concentration of CST−AuNPs was 3.637 nanomolar [nM] calculated using Beer's law according to the extinction coefficient on particle diameter (ε = 7.19 × 10^9 M^{-1} cm^{-1} for the particle size of CST−AuNPs = 2.41 nm). For references, the extinction coefficient for CST−AuNPs is calculated using the following equation of ln ε = 1.4418 ln$D$ + 18.955 and D is the diameter in nanometer (nm).[29]

2.4. Characterization. Ultraviolet−visible (UV−vis) absorption spectra of AuNPs were measured using a double-beam UV1800 (Shimadzu, China) spectrophotometer with a 1 cm path length quartz cuvette. All the measurements were repeated at least three times. The morphology, particle size, and distribution of AuNPs were photographed using a transmission electron microscope (TEM, JEM−2010 model, JEOL Co., Ltd. Japan) at an accelerating voltage of 200 kV. Zeta potential of NPs was measured using a Nano ZS−Malvern instrument, England with a 633 nm helium−neon laser. An X-ray diffractometer was used to analyze the crystallographic structure of the NPs. The XRD patterns were recorded over a 2θ (Smartlab SE diffractometer, RIGAKU, Japan). pH of the synthesized solution was adjusted using a benchtop pH meter (Mettler)

2.5. Antimicrobial Assay. The antimicrobial activity of chitosan, CST, and CST−AuNPs against *S. mutans* ATCC 25175 and *S. sobrinus* ATCC 33402 was evaluated by the agar well diffusion method and macrodilution method.

2.5.1. Agar Well Diffusion Assay. The 10^4 CFU/mL of inoculum was swapped onto Mueller−Hinton agar plates;

https://doi.org/10.1021/acsomega.2c02776
ACS Omega 2022, 7, 26582−26590

afterward, a well with a size of 5 mm was cut in the agar plate. Each well was aseptically filled up with 20 μL of (a) Control: prepared by mixing 1% v/v CH_3COOH with 4% w/v of Tween80, (b) Chitosan: prepared by dissolving 1% w/v of chitosan pH 4.5 in control solution), (c) CST: prepared by dissolving 1% w/v of CST pH 4.5 in control solution, and (d) CST−AuNPs: prepared by dissolving pH 9.0 of AuNPs coated with $CST_{0.020\%w/v}$ mixed with 4% w/v of Tween80. The plates were incubated at 37 °C for 24 h. 4% of Tween 80 was introduced as controls. The diameter of the inhibition zone around each well was measured and expressed in the mean diameter of the inhibition zone in millimeters (n = 3).

2.5.2. Minimum Inhibitory Concentration (MIC) and Minimum Bactericidal Concentration (MBC) Assay. MIC and MBC values were determined by broth macrodilution assay. Colonies of the same morphological type were selected and transferred to 0.85% w/v of sterile saline. To achieve the turbidity of a 0.5 McFarland standard, inoculum was diluted with Brain Heart Infusion broth 1:200 (approximately 5×10^5 CFU/mL). Each stock as-synthesized chitosan, CST, and CST−AuNPs were dissolved in 4% w/v of tween 80 with the final concentration ranging from 0.40 to 200 mg/L. Then, 50 μL of adjusted *S. mutans* ATCC 25175 and *S. sobrinus* ATCC 33402 were added into each tube. After that, the samples were incubated overnight at 37 °C for 24 h. MICs and MBCs were evaluated by no visible growth of bacteria and lowest concentration of an antimicrobial agent that kills 99.9% of the initial bacterial population method, respectively.

3. RESULTS AND DISCUSSION

3.1. Synthesis and Characterization of CST. To graft thymol onto the chitosan side chain, the Mannich reaction was

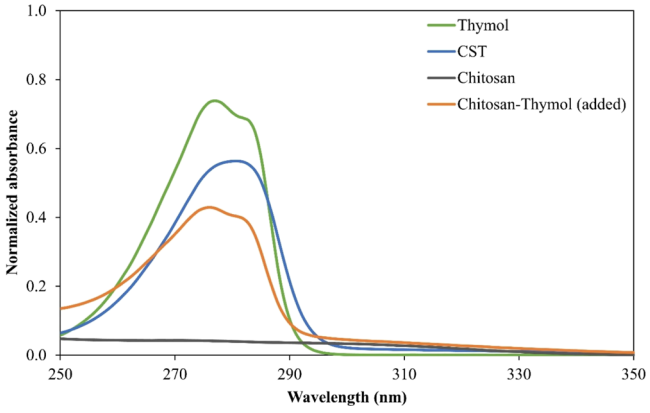

Figure 2. UV−vis spectra of CST, chitosan, thymol, and chitosan mixed with 0.05% w/v thymol in 0.1 M HCl solution.

used in the experimental step. An amino group of chitosan can react with formaldehyde to form an electrophile imine compound (−N═CH_2) and then react with attached by introducing at the para position of the phenol group to yield secondary amines or benzylamine. Thus, chitosan could be grafted with thymol through the carbene bridge. The synthesis pathway of CST is shown in Scheme 1a. The product was structurally characterized by ^{1}H NMR as shown in Figure 1. The chitosan spectra showed characteristic peaks at 1.86 and 2.97 ppm assigned to H_7 and H_2, respectively. The peaks at 3.25−4.02 ppm were assigned to H_3−H_6 and $H_{2'}$−$H_{6'}$. In terms of CST, it showed a characteristic peak of chitosan and

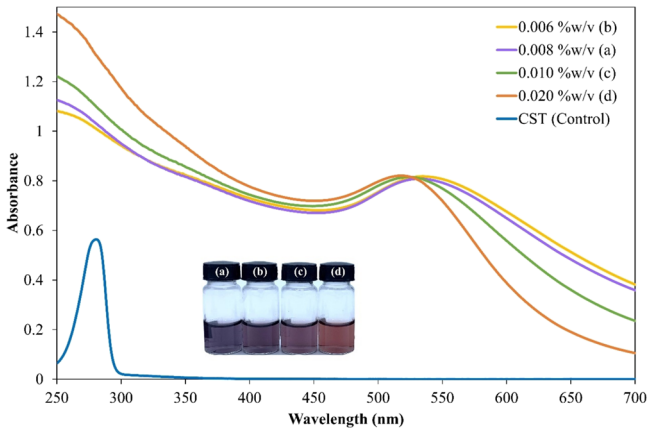

Figure 3. Visual observation and absorption spectra of CST coated on gold nanoparticles with various concentrations of CST (a) 0.006%w/v, (b) 0.008%w/v, (c) 0.010%w/v, and (d) 0.020%w/v and CST as the control on the synthesis step.

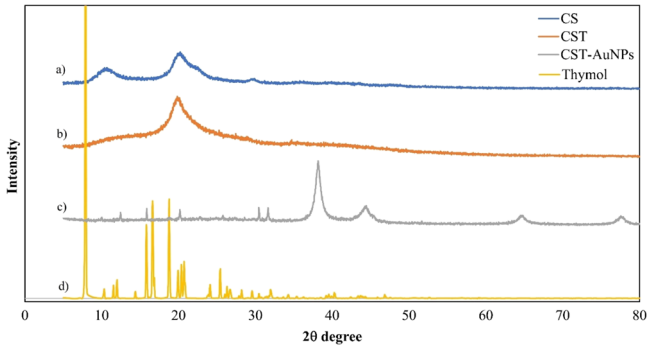

Figure 4. XRD pattern of (a) chitosan, (b) CST, (c) CST coated on gold nanoparticles, and (d) thymol.

found new peaks at 1.00 and 2.15 ppm which correspond to protons of the methyl group of thymol (H_f and H_b), respectively. Moreover, the doublet peaks around 6.74 and 7.10 ppm of aromatic protons of thymol (H_c and H_d) were also observed, respectively. Thus, it was indicated that thymol was successfully grafted onto chitosan through the Mannich reaction. The degree of substitution of CST was 10.0%, as calculated from the ^{1}H NMR data. For EA results, the C/N ratio of CST was higher than that of chitosan, indicating that additional carbon atoms existed after the reaction. The data also revealed that the degree of substitution value ($\%DS_{EA}$) was 9.2% (Table S1, Supporting Information).

The UV−vis spectra of chitosan, CST, thymol, and chitosan mixed thymol are displayed in Figure 2. It was found that the chitosan spectrum did not show any peak ranging from 250 to 350 nm while CST spectra exhibited broad peaks at 281 nm corresponding to the aromatic structure of thymol. Comparison with the spectra of chitosan mixed thymol which showed absorption peaks at 276 and 282 nm, corresponding to the characteristic peak of thymol, the CST spectra showed a red shift phenomenon implying chemical modification on thymol molecules.[30] The results suggested that thymol was grafted onto the chitosan backbone.

3.2. Synthesis and Characterization of CST Coated on the Gold Nanoparticle Surface. Our main motivation in this work was to produce AuNPs using CST as the capping agent. The capping agent is needed to prevent the growth of the nanoparticles (NPs). This process occurs during the

https://doi.org/10.1021/acsomega.2c02776
ACS Omega 2022, 7, 26582−26590

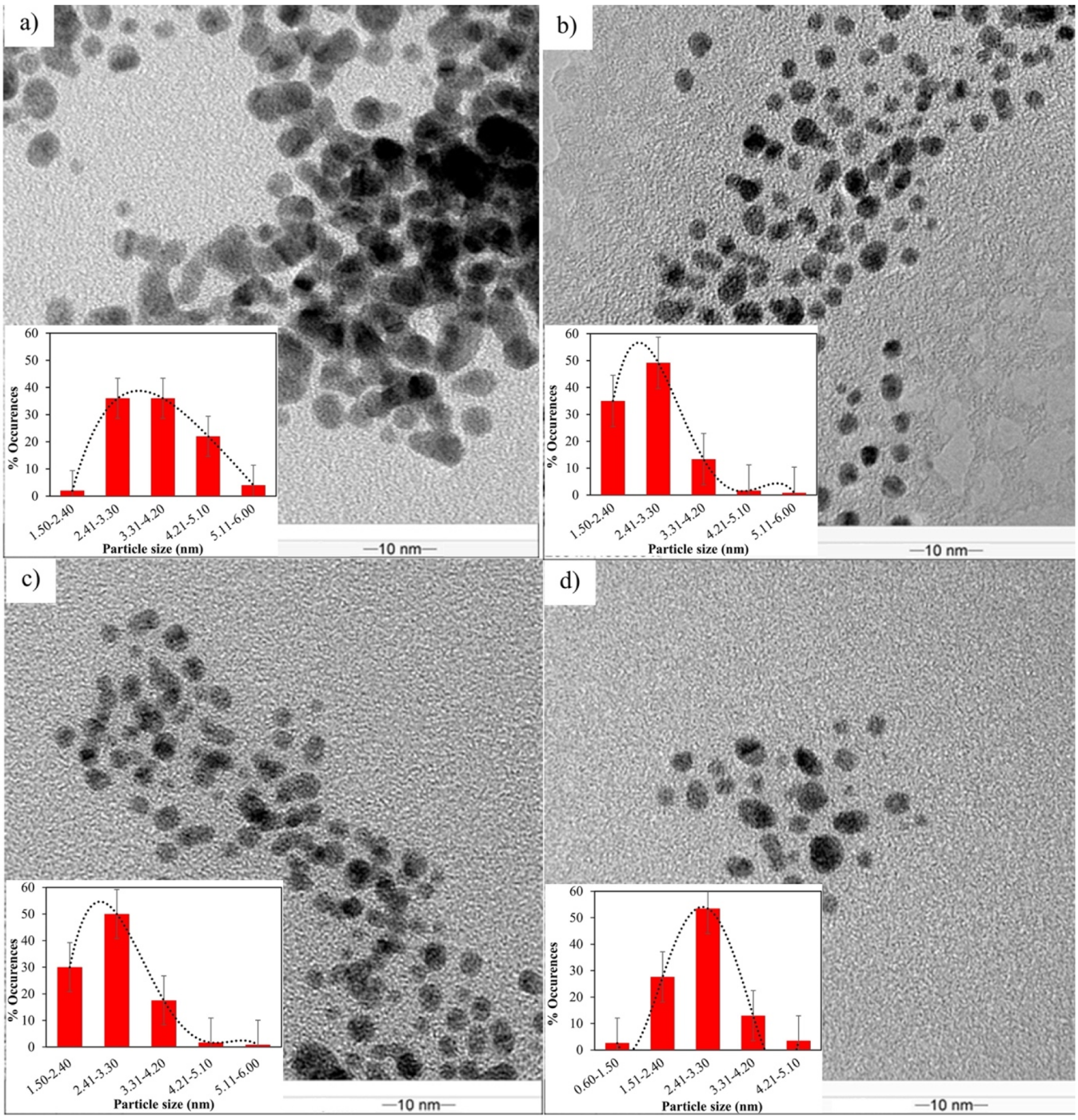

Figure 5. TEM images and size distribution of CST coated on gold nanoparticles at a CST concentration of (a) 0.006% w/v, (b) 0.008% w/v, (c) 0.01% w/v, and (d) 0.02% w/v.

formation of the NPs when a capping agent adsorbs at the NP surface. In the present case, CST-modified AuNPs were synthesized according to a very simple and rapid chemical method as shown in Scheme 1b. The synthesis of AuNPs with CST can be achieved through chemical reduction with $NaBH_4$ as a reducing agent. Au^{3+} ions were reduced to Au^0 in the presence of CST as a capping agent obtaining stable AuNPs. A zeta potential analyzer has been used to clarify the stability of NPs. Zeta potential analysis (Figure S1, Supporting Information) demonstrated that the as-synthesized CST−AuNPs had negative potential (pH = 9), which can prevent nanoparticle−nanoparticle aggregation and be dispersed from each other in the aqueous phase.

To study the influence of CST concentration for AuNP synthesis, four different CST concentrations of 0.006, 0.008, 0.010, and 0.020% w/v were used for investigation. The visual observation and absorption characteristics of various concentrations of AuNPs stabilized with CST are shown in Figure 3. The AuNPs formed in the solution, through nucleation growth, displayed a characteristic of vivid blue to dark red color when the concentration of CST increased from 0.006−0.020% w/v. Indeed, when the concentration of CST increased from 0.006−0.020%, the absorption spectra shifted to blue-

https://doi.org/10.1021/acsomega.2c02776
ACS Omega 2022, 7, 26582−26590

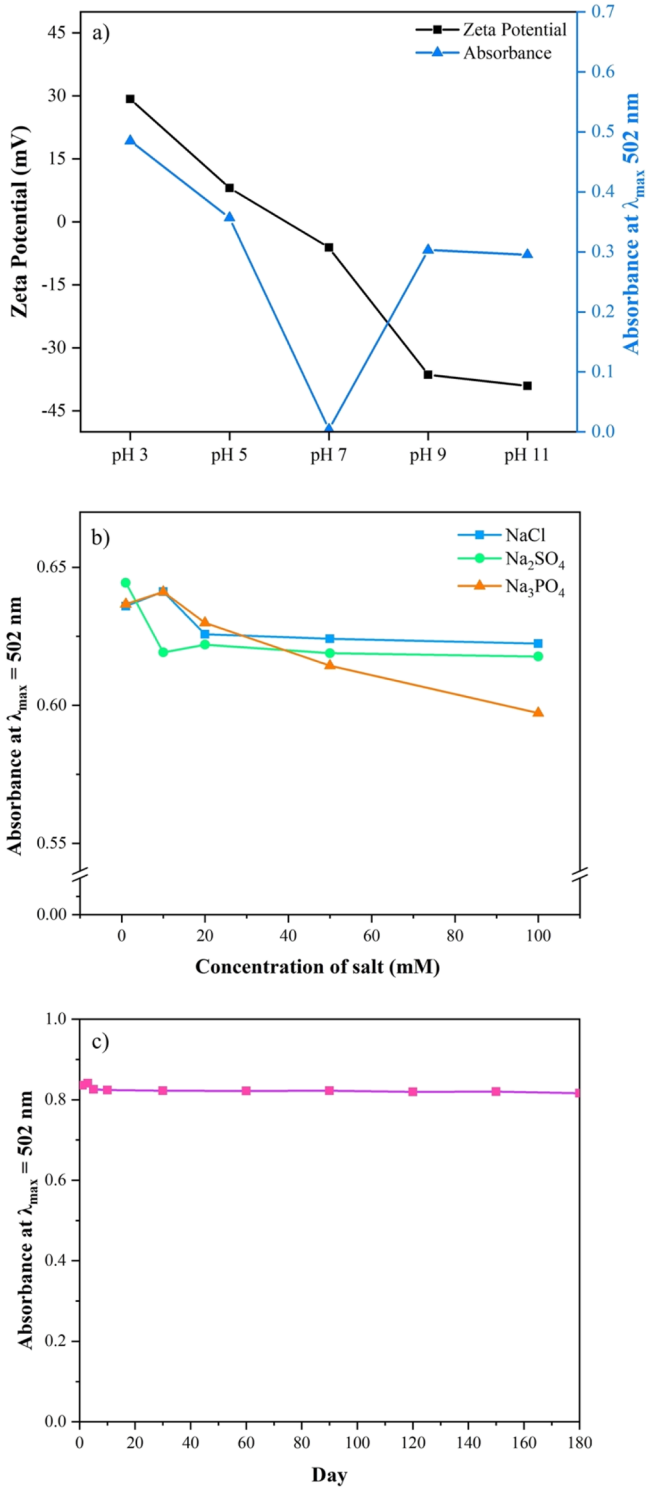

Figure 6. Effect of (a) pH, (b) ionic strength, and (c) time on the stability of CST coated on gold nanoparticles.

shift due to the surface plasmon resonance phenomenon. The extinction spectrum of $CST_{0.020\%w/v}$ − AuNPs exhibited a single peak around 502 nm with the zeta potential at pH 9 of −33.8 mV.

To further confirm the successful formation of CST−AuNPs, XRD measurements were carried out in order to identify the crystallinity structure of the NPs, and corresponding XRD patterns are shown in Figure 4. CST−AuNPs

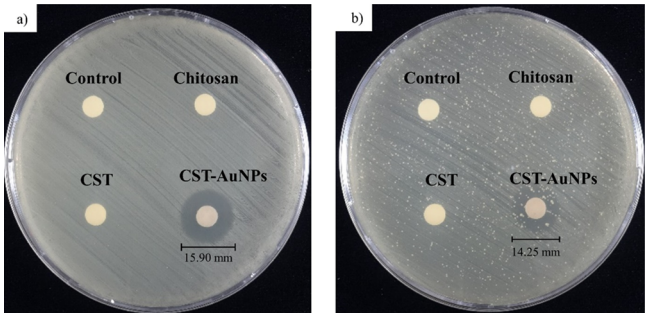

Figure 7. Bacterial inhibition photographs of chitosan, CST, and CST coated on gold nanoparticles and control against using the agar well diffusion method (a) *S. mutans* and (b) *S. sobrinus*.

Table 1. MICs and MBCs of Chitosan, CST, and CST Coated on Gold Nanoparticles against *S. mutans* and *S. sobrinus*

synthesis materials	*S.mutans* ATCC 25175		*S. sobrinus* ATCC 33402	
	MIC (mg/L)	MBC (mg/L)	MIC (mg/L)	MBC (mg/L)
chitosan	100	100	100	100
CST	50	50	50	50
CST−AuNPs	25	100	100	200

exhibited four distinct peaks corresponding to standard Bragg reflections. The 2θ (Bragg reflections) values are 38.1(111), 44.3(200), 64.5(220), and 77.7(311) of the face centered cubic (FCC) lattice. The potent diffraction at 38.1 peak shows that the preferred growth orientation of zero valent gold was fixed in the (111) direction.[31] These experimental observations clearly demonstrate that AuNP capping with CST was found to be in agreement with the literature report.[8]

To examine the size and particle morphology, TEM analysis was performed. As shown in Figure 5, the effect of CST concentration onto the preparation of AuNPs has been studied. The concentration of $HAuCl_4{\cdot}3H_2O$ was kept constant at 1 mM in the synthesis step, and different batches were prepared with CST concentration increasing from 0.006 to 0.02% w/v. The TEM images show that AuNPs are nanosize in shape and well dispersed in aqueous media. The particle size of AuNP capping with different CST concentrations from 0.006 to 0.02% w/v was found in the range of 1.50−5.10 nm. The particle size of CST−AuNPs was found to be not statistically significant different. The appropriate concentration of CST for AuNP synthesis was found at 0.020%w/v showing a particle size of 2.41−3.30 nM. This observation suggested that CST played a role as a stabilizing agent to provide a good dispersion state of the AuNPs.

3.3. Stability of CST Coated on the Gold Nanoparticle Surface. The stability of CST−AuNPs under various conditions was also investigated. The results are shown in Figure 6. It is well known that chitosan was soluble under acid conditions due to the protonation of amino groups on the chitosan backbone. The derivatives of CST could be dissolved under acid conditions at about pH < 5. The pH values of the CST would affect the interaction of AuNPs conjugated with CST. Therefore, it was necessary to investigate the effect of pH values on the stability of CST−AuNPs. Figure 6a shows the UV−visible absorbance at λ_{max} of 502 nm of CST−AuNPs when varying pH from 3−11. CST−AuNPs could be dispersed

https://doi.org/10.1021/acsomega.2c02776
ACS Omega 2022, 7, 26582−26590

Table 2. Comparison of Antibacterial Properties of Metallic Nanoparticles

method	microorganism	inhibition zone (mm)	MIC (mg/L)	MBC (mg/L)	ref.
peptide (extracted from Vespa orientalis waspvenom) −AuNPs	*S. mutans*	14.71	18.78	32	34
chitosan gel − AuNPs	*S. mutans*	8.56			35
lycopene − AgNPs	*S. aureus*	12			36
	S. mutans	12			
Aspergillus terreus IF0 − AuNPs	*E. coli*	13			37
	S. mutans	Not Active			
CST−AuNPs	*S. mutans* ATCC 25175	15.90	25	100	Present work
	S. sobrinus ATCC 33402	14.25	100	200	

in pH less than 5 and higher than 7 whereas the precipitation occurred at pH 7. As a result of the addition of $NaBH_4$, the pH solution was 9, and the solution was well dispersed, as reported in several studies.[32,33] Adjusting pH to basic range seemed to have no effect on their stability. When the pH was changed to acidity (pH 7), however, all particles precipitated. This could be because the electrostatic repulsion of negatively charged BO^{3-} has been destroyed, and deprotonated CST has no charge (zeta potential value near zero), causing AuNPs to precipitate. In a more acidic solution (pH 3), the amino groups of CST were protonated, making it more positively charged (corresponding to a higher zeta potential value) and causing AuNPs to have good dispersion.

Another important parameter for the stability of CST−AuNPs is ionic strength. The stability of CST−AuNPs as a function of salt concentration and salt type such as NaCl, Na_2SO_4, and Na_3PO_4 was investigated (Figure 6b). At low salt concentration, CST−AuNPs showed higher stability more than that at high concentration. The monovalent (Cl^-) and divalent (SO_4^{2-}) showed the slow precipitation of CST−AuNPs, while for trivalent (PO_4^{3-}), the CST−AuNP colloid tends to precipitate the fastest. The precipitation could be attributed to the lower of the electrostatic repulsion between CST and AuNPs and thus lead to the aggregation and sedimentation of AuNPs.

Figure 6c showed the effect of time onto the stability of CST−AuNPs. CST−AuNPs with pH 9 can be more stable more than 3 months.

3.4. Antimicrobial Assay. *3.4.1. Agar Well Diffusion Assay.* The antibacterial activity of CST−AuNPs was assessed by the agar well diffusion method. The results are shown in Figure 7. The CST−AuNPs showed good antibacterial activity against almost all pathogenic bacteria. The tuning of the capping agent used in the synthesis step strongly influences latter antimicrobial activity of the NPs against *S. mutans* ATCC 25175 and *S. sobrinus* ATCC 33402, with an inhibition clear zone of 15.90 and 14.25 mm against *S. mutans* and *S. sobrinus*, respectively. Indicated AuNPs show antibacterial properties when CST binds with the AuNP surface.

3.4.2. MIC and MBC Assay. The antibacterial activity of chitosan, CST, and CST−AuNPs against the bacterial strains was assessed by MIC and MBC. MIC and MBC values for CS, CST, and CST−AuNPs against *S. mutans* ATCC 25175 and *S. sobrinus* ATCC 33402 are shown in Table 1. The MICs and MBCs of CST−AuNPs against *S. mutans* ATCC 25175 were found to be 25 and 100 mg/L, respectively, while *S. sobrinus* ATCC 33402 was found to have an MIC and MBC of 100 and 200 mg/L, respectively. The report indicated that CST−AuNPs exhibited antibacterial activity against both bacterial species. Therefore, the modification of thymol into the backbone of chitosan was considered essential for antimicrobial activity enhancement.

Metallic nanoparticles have been widely studied and applied as an effective antibacterial agent. The antibacterial properties of modified metallic nanoparticles in the previous study are shown in Table 2. According to our proposed method, CST−AuNPs can be deemed to have potential with strong antimicrobial activity. CST coated on the AuNP surface can thus be employed as an antibacterial agent in a variety of biological applications.

4. CONCLUSIONS

A novel control of cariogenic bacteria in the oral cavity was made from a simple chemical reduction method using CST coated on the AuNP surface. The grafting of thymol onto the chitosan backbone was synthesized through adapting the Mannich reaction which provided degree of substitution values ($\%DS_{NMR}$) of 10.0%. Excellent properties of CST are very effective in stabilization of AuNPs. The electrostatic properties of CST were used to primarily provide the stabilization of the AuNPs by electrostatic repulsion. The particles of AuNPs were found to be well dispersed and mostly spherical in shape with an average particle size of 2.41−3.30 nm. The presence of AuNPs with CST enhanced bactericidal activity against *S. mutans* ATCC 25175 and *S. sobrinus* ATCC 33402. This CST coated on the AuNP surface potentially constitutes an important new weapon in the fight of cariogenic bacteria-related infection.

■ ASSOCIATED CONTENT

Supporting Information

The Supporting Information is available free of charge at https://pubs.acs.org/doi/10.1021/acsomega.2c02776.

Table S1: The elemental content of carbon, hydrogen, and nitrogen in chitosan, thymol, and CST calculated using EA and Figure S1: The zeta potential of CST coated on gold nanoparticles (pH 9) with various concentrations of CST (0.006, 0.008, 0.010, and 0.020% w/v) (PDF)

■ AUTHOR INFORMATION

Corresponding Authors

Ekarat Detsri − *Department of Chemistry, School of Science and Integrated Applied Chemistry Research Unit, School of Science, King Mongkut's Institute of Technology Ladkrabang, Bangkok 10520, Thailand;* orcid.org/0000-0001-8627-0631; Email: Ekarat.de@kmitl.ac.th

Pathavuth Monvisade − *Department of Chemistry, School of Science and Polymer Synthesis and Functional Materials*

https://doi.org/10.1021/acsomega.2c02776
ACS Omega 2022, 7, 26582−26590

Research Unit, School of Science, King Mongkut's Institute of Technology Ladkrabang, Bangkok 10520, Thailand; Email: Pathavuth.mo@kmitl.ac.th

Authors

Pakawat Chittratan − *Department of Chemistry, School of Science and Polymer Synthesis and Functional Materials Research Unit, School of Science, King Mongkut's Institute of Technology Ladkrabang, Bangkok 10520, Thailand*

Jongjit Chalitangkoon − *Department of Chemistry, School of Science and Polymer Synthesis and Functional Materials Research Unit, School of Science, King Mongkut's Institute of Technology Ladkrabang, Bangkok 10520, Thailand;* orcid.org/0000-0002-2836-125X

Karn Wongsariya − *Department of Biology School of Science, King Mongkut's Institute of Technology Ladkrabang, Bangkok 10520, Thailand*

Arjnarong Mathaweesansurn − *Department of Chemistry, School of Science and Applied Analytical Chemistry Research Unit, School of Science, King Mongkut's Institute of Technology Ladkrabang, Bangkok 10520, Thailand*

Complete contact information is available at: https://pubs.acs.org/10.1021/acsomega.2c02776

Notes

The authors declare no competing financial interest.

■ ACKNOWLEDGMENTS

This work has received funding support from the National Science, Research and Innovation Fund (NSRF), The Royal Golden Jubilee (RGJ) Ph.D. Programme (Grant No. PHD/0080/2559), and King Mongkut's Institute of Technology Ladkrabang (KMITL), grant number KREF016005. The authors would like to thank the Scientific Instruments Center, School of Science, King Mongkut's Institute of Technology Ladkrabang for supporting the instruments.

■ REFERENCES

(1) Liu, J.; Ling, J.-Q.; Zhang, K.; Huo, L.-J.; Ning, Y. Effect of Sodium Fluoride, Ampicillin, and Chlorhexidine on Streptococcus mutans Biofilm Detachment. *Antimicrob. Agents Chemother.* **2012**, *56*, 4532−4535.

(2) Al-Ahmad, A.; Wiedmann-Al-Ahmad, M.; Auschill, T. M.; Follo, M.; Braun, G.; Hellwig, E.; Arweiler, N. B. Effects of commonly used food preservatives on biofilm formation of Streptococcus mutans in vitro. *Arch. Oral Biol.* **2008**, *53*, 765−772.

(3) Thomas, A.; Thakur, S.; Mhambrey, S. Comparison of the antimicrobial efficacy of chlorhexidine, sodium fluoride, fluoride with essential oils, alum, green tea, and garlic with lime mouth rinses on cariogenic microbes. *J. Int. Soc. Prev. Community Dent.* **2015**, *5*, 302−308.

(4) Solanki, L. A.; Shantha Sundari, K. K.; Rajeshkumar, S. In-vitro Cytotoxicity Evaluation of Green Synthesized Gold Nanoparticles and Its Indigenous Mouthwash. *J. Pure Appl. Microbiol.* **2021**, *15*, 735−742.

(5) Solanki, L.; Shantha Sundari, K.; Muralidharan, N.; Jain, R. Antimicrobial effect of novel gold nanoparticle oral rinse in subjects undergoing orthodontic treatment: An ex-vivo study. *J. Int. Oral Health.* **2022**, *14*, 47−52.

(6) Ahrari, F.; Eslami, N.; Rajabi, O.; Ghazvini, K.; Barati, S. The antimicrobial sensitivity of Streptococcus mutans and Streptococcus sangius to colloidal solutions of different nanoparticles applied as mouthwashes. *Dent. Res. J. (Isfahan)* **2015**, *12*, 44−49.

(7) Chamundeeswari, M.; Sobhana, S. S. L.; Jacob, J. P.; Kumar, M. G.; Devi, M. P.; Sastry, T. P.; Mandal, A. B. Preparation, characterization and evaluation of a biopolymeric gold nanocomposite with antimicrobial activity. *Biotechnol. Appl. Biochem.* **2010**, *55*, 29−35.

(8) Franconetti, A.; Carnerero, J. M.; Prado-Gotor, R.; Cabrera-Escribano, F.; Jaime, C. Chitosan as a capping agent: Insights on the stabilization of gold nanoparticles. *Carbohydr. Polym.* **2019**, *207*, 806−814.

(9) Dykman, L. A.; Khlebtsov, N. G. Gold nanoparticles in biology and medicine: recent advances and prospects. *Acta Naturae* **2011**, *3*, 34−55.

(10) Regiel-Futyra, A.; Kus-Liśkiewicz, M.; Sebastian, V.; Irusta, S.; Arruebo, M.; Stochel, G.; Kyzioł, A. Development of Noncytotoxic Chitosan−Gold Nanocomposites as Efficient Antibacterial Materials. *ACS Appl. Mater. Interfaces* **2015**, *7*, 1087−1099.

(11) Abrica-González, P.; Zamora-Justo, J. A.; Sotelo-López, A.; Vázquez-Martínez, G. R.; Balderas-López, J. A.; Muñoz-Diosdado, A.; Ibáñez-Hernández, M. Gold nanoparticles with chitosan, N-acylated chitosan, and chitosan oligosaccharide as DNA carriers. *Nanoscale Res. Lett.* **2019**, *14*, 258.

(12) Su, C.; Huang, K.; Li, H.-H.; Lu, Y.-G.; Zheng, D.-L. Antibacterial Properties of Functionalized Gold Nanoparticles and Their Application in Oral Biology. *J. Nanomater.* **2020**, *2020*, No. 5616379.

(13) Darabpour, E.; Kashef, N.; Amini, S. M.; Kharrazi, S.; Djavid, G. E. Fast and effective photodynamic inactivation of 4-day-old biofilm of methicillin-resistant Staphylococcus aureus using methylene blue-conjugated gold nanoparticles. *J. Drug Deliv. Sci. Technol.* **2017**, *37*, 134−140.

(14) Singh, P.; Pandit, S.; Garnæs, J.; Tunjic, S.; Mokkapati, V. R.; Sultan, A.; Thygesen, A.; Mackevica, A.; Mateiu, R. V.; Daugaard, A. E.; Baun, A.; Mijakovic, I. Green synthesis of gold and silver nanoparticles from Cannabis sativa (industrial hemp) and their capacity for biofilm inhibition. *Int. J. Nanomed.* **2018**, *13*, 3571−3591.

(15) Zhao, Y.; Tian, Y.; Cui, Y.; Liu, W.; Ma, W.; Jiang, X. Small Molecule-Capped Gold Nanoparticles as Potent Antibacterial Agents That Target Gram-Negative Bacteria. *J. Am. Chem. Soc.* **2010**, *132*, 12349−12356.

(16) Chávez de Paz, L. E.; Resin, A.; Howard, K. A.; Sutherland, D. S.; Wejse, P. L. Antimicrobial effect of chitosan nanoparticles on streptococcus mutans biofilms. *Appl. Environ. Microbiol.* **2011**, *77*, 3892−3895.

(17) Costa, E. M.; Silva, S.; Costa, M. R.; Pereira, M.; Campos, D. A.; Odila, J.; Madureira, A. R.; Cardelle-Cobas, A.; Tavaria, F. K.; Rodrigues, A. S.; et al. Chitosan mouthwash: Toxicity and in vivo validation. *Carbohydr. Polym.* **2014**, *111*, 385−392.

(18) Uraz, A.; Boynueğri, D.; Özcan, G.; Karaduman, B.; Uç, D.; Şenel, S.; Pehlivan, S.; Öğüs, E.; Sultan, N. Two percent chitosan mouthwash: A microbiological and clinical comparative study. *J. Dent. Sci.* **2012**, *7*, 342−349.

(19) Liu, X.; Xia, W.; Jiang, Q.; Yu, P.; Yue, L. Chitosan oligosaccharide-N-chlorokojic acid mannich base polymer as a potential antibacterial material. *Carbohydr. Polym.* **2018**, *182*, 225−234.

(20) Khan, S. T.; Khan, M.; Ahmad, J.; Wahab, R.; Abd-Elkader, O. H.; Musarrat, J.; Alkhathlan, H. Z.; Al-Kedhairy, A. A. Thymol and carvacrol induce autolysis, stress, growth inhibition and reduce the biofilm formation by Streptococcus mutans. *AMB Express* **2017**, *7*, 49.

(21) Marchese, A.; Orhan, I. E.; Daglia, M.; Barbieri, R.; Di Lorenzo, A.; Nabavi, S. F.; Gortzi, O.; Izadi, M.; Nabavi, S. M. Antibacterial and antifungal activities of thymol: A brief review of the literature. *Food Chem.* **2016**, *210*, 402−414.

(22) Nagoor Meeran, M. F.; Javed, H.; Al Taee, H.; Azimullah, S.; Ojha, S. K. Pharmacological Properties and Molecular Mechanisms of Thymol: Prospects for Its Therapeutic Potential and Pharmaceutical Development. *Front. Pharmacol.* **2017**, *8*, 380.

(23) Chalitangkoon, J.; Monvisade, P. Dual pH/thermal-dependent coloring polymeric dye through Mannich reaction of chitosan: Synthesis and characterization. *Carbohydr. Polym.* **2019**, *223*, No. 115049.

(24) Wang, W.; Meng, Q.; Li, Q.; Liu, J.; Zhou, M.; Jin, Z.; Zhao, K. Chitosan Derivatives and Their Application in Biomedicine. *Int. J. Mol. Sci.* **2020**, *21*, 487.
(25) Yin, M.; Wang, Y.; Zhang, Y.; Ren, X.; Qiu, Y.; Huang, T.-S. Novel quaternarized N-halamine chitosan and polyvinyl alcohol nanofibrous membranes as hemostatic materials with excellent antibacterial properties. *Carbohydr. Polym.* **2020**, *232*, No. 115823.
(26) Yue, L.; Sun, D.; Mahmood Khan, I.; Liu, X.; Jiang, Q.; Xia, W. Cinnamyl alcohol modified chitosan oligosaccharide for enhancing antimicrobial activity. *Food Chem.* **2020**, *309*, No. 125513.
(27) Khan, A.; Alamry, K. A. Recent advances of emerging green chitosan-based biomaterials with potential biomedical applications: A review. *Carbohydr. Res.* **2021**, *506*, No. 108368.
(28) Chalitangkoon, J.; Monvisade, P. Synthesis of chitosan-based polymeric dyes as colorimetric pH-sensing materials: Potential for food and biomedical applications. *Carbohydr. Polym.* **2021**, *260*, No. 117836.
(29) Detsri, E.; Seeharaj, P.; Sriwong, C. A sensitive and selective colorimetric sensor for reduced glutathione detection based on silver triangular nanoplates conjugated with gallic acid. *Colloids Surf. A Physicochem. Eng. Asp.* **2018**, *541*, 36−42.
(30) Yu, S.; Du, J.; Zheng, Y.; Yan, L. Synthesis and characterization of carboxymethyl chitosan containing functional ultraviolet absorber substituent. *J. Appl. Polym. Sci.* **2007**, *106*, 4098−4103.
(31) Sneha, K.; Esterle, A.; Sharma, N.; Sahi, S. Yucca-derived synthesis of gold nanomaterial and their catalytic potential. *Nanoscale Res. Lett.* **2014**, *9*, 627.
(32) Adlim, A.; Bakar, M. A. Preparation of chitosan-gold nanoparticles: part 1 (of 2). Effect of reducing technique. *Indones. J. Chem.* **2008**, *8*, 184−188.
(33) Adlim, A. Preparation of Chitosan-Stabilized Silver (Chi-Ag) Nanoparticles Using Different Reducing Agents And Techniques. *J. Sains Tek.* **2006**, *12*, 185−191.
(34) Jalaei, J.; Layeghi-Ghalehsoukhteh, S.; Hosseini, A.; Fazeli, M. Antibacterial effects of gold nanoparticles functionalized with the extracted peptide from Vespa orientalis wasp venom. *J. Pept. Sci.* **2018**, *24*, No. e3124.
(35) Sámano-Valencia, C.; Martínez-Castañón, G. A.; Martínez-Gutiérrez, F.; Ruiz, F.; Toro-Vázquez, J. F.; Morales-Rueda, J. A.; Espinosa-Cristóbal, L. F.; Zavala Alonso, N. V.; Niño Martínez, N. Characterization and Biocompatibility of Chitosan Gels with Silver and Gold Nanoparticles. *J. Nanomater.* **2014**, *2014*, 1−11.
(36) Murthykumar, K.; Malaiappan, S.; Shanmugam, R. Antioxidant and antibacterial effect of lycopene mediated silver nanoparticle against Staphylococcus aureus and Streptococcus mutans- an In vitro study. *Plant Cell Biotechnol. Mol. Biol.* **2020**, *21*, 90−98.
(37) Priyadarshini, E.; Pradhan, N.; Sukla, L. B.; Panda, P. K. Controlled Synthesis of Gold Nanoparticles UsingAspergillus terreusIF0 and Its Antibacterial Potential against Gram Negative Pathogenic Bacteria. *J. Nanotechnol.* **2014**, *2014*, 1−9.

https://doi.org/10.1021/acsomega.2c02776
ACS Omega 2022, 7, 26582−26590